Research Article

Journal of Environmental Nanotechnology

Development and Characterization of an Eco-friendly Stishovite Clay-manganese Dioxide Nanocomposite for Efficient Dye Removal from Wastewater

K. Prabhakaran[1*], T. Mohanapriya[2], M. G. Geena[3] and E. Kavitha[4]

[1]Center for Environmental Research, Department of Chemistry, Kongu Engineering College, Perundurai, Erode, TN, India
[2]Department of Chemistry, Erode Arts and Science College, Erode, TN, India
[3]Department of Agriculture Engineering, Dhanalakshmi Srinivasan University, Trichy, TN, India
[4]Department of Civil Engineering, Aishwarya College of Engineering and Technology, Bhavani, Erode, TN, India
Received: 14.10.2024 Accepted: 20.12.2024 Published: 30.12.2024
*prabhakaranchemist@gmail.com

ABSTRACT

The contamination of water bodies with artificial dyes causes serious health and ecologicalconcerns. The discharge of dyes into water systems from various industries, including textiles, paper, and others, causes significant ecological disturbances and poses health risks to humans. This study deals with the development of eco-friendly Nano composite made with stishovite clay and MnO_2 for the purpose of removing dye pollutants from wastewater through adsorption. The composite's adsorptive capabilities are improved by the addition of MnO_2, while the stishovite clay serves as a stable matrix. The various material characterization technique was employed both stishovite clay and Nano composite sample. X-ray diffarction (XRD), scanning electron microscopy (SEM), transmission electron microscopy (TEM), and Brunauer-Emmett-Teller (BET) analysis were all employed to characterize the nanocomposite thoroughly. XRD confirmed the presence of crystals, whereas FT-IR revealed excellent incorporation of MnO_2, with vibrational peaks unique to the composite structure. SEM and TEM revealed improved surface shape and dispersion of MnO_2 nanoparticles, leading to an increase in surface area. The BET study demonstrated a substantial increase in both the pore volume and surface area, a critical factor in the enhancement of dye adsorption capability. According to the results, the stishovite-MnO_2 nanocomposite is a long-term, environmentally friendly, and very effective way to deal with dye pollution.

Keywords: Stishovite clay; Manganese dioxide (MnO_2); Nanocomposite; Dye removal; Eco-friendly synthesis.

1. INTRODUCTION

The enormous industrialization of the current century has presented substantial environmental issues, notably in the management of wastewater that contains hazardous contaminants. Specifically, man-made dyes utilised in leather, textile, paper, and cosmetic sectors pose significant challenges because of their intricate chemical compositions, which are resistant to biodegradation and persist in the environment for prolonged period of time (Chitradevi *et al.* 2021; Younis *et al.* 2021; Arunvivek*et al.* 2014). These pigments not only provide colour to bodies of water but also obstruct the passage of sunlight, therefore disturbing aquatic ecosystems and causing a decrease in oxygen levels in the drinking water (Saad and Atia, 2014). Furthermore, numerous dyes have poisonous, mutagenic, or carcinogenic properties, so presenting significant hazards to both human health and the atmosphere (Gupta and Suhas, 2009). The textile industry generates significant quantities of chemicals that are exceedingly hazardous, and these chemicals are subsequently released at various phases of the processing lifecycle (Kishor *et al.* 2021). Moreover, it is widely recognized that textile dyes, if not adequately processed, pose substantial eco-toxicological risks to living species (Garg and Tripathi, 2017; Parmar *et al.* 2022; Lou *et al.* 2021; Adesanmi*et al.* 2022). The detrimental effects of untreated wastewater on ecological systems and the corresponding health hazards for human populations have been extensively documented in numerous research.

Traditional approaches to dye removal, such as coagulation, flocculation, and biological treatment, are generally inadequate because they cannot fully break down or eliminate dye molecules from waste water (Al-Tohamy *et al.* 2022). The treatment of wastewater from textile factories has been the subject of numerous developments in recent years. These methods include membrane filtration (Raval *et al.* 2022), ozonation (Shajeelammal*et al.* 2022), biosorption (El-Kassimi *et al.* 2021), electro coagulation (Moneer *et al.* 2021), photo catalytic removal (Khan and Pathak, 2020), advanced oxidation process (Zupko *et al.* 2020), coagulation and flocculation (Januário *et al.* 2021), electrochemical precipitation, magnetic biocoagulant (Alahmadi, 2022), electroflotation (Talaiekhozani *et al.* 2020), CNT composites (Yadav *et al.* 2021), ultrafiltration (Benkhaya

et al. 2020), nanofibers (Ebrahimi *et al.* 2022), nanotubes (Zhao *et al.* 2022), membrane filtration (Xiang *et al.* 2022), nanocomposite hydrogels (Jana *et al.* 2019), catalytic photo degradation (Cardona *et al.* 2022; Roa *et al.* 2021), Biochar composite (Ismadji *et al.* 2016).

Nevertheless, adsorption is widely acknowledged as a very efficient and versatile technique for eliminating dyes, offering advantages such as low operational costs, simplicity, and immense efficacy (Mudhoo *et al.* 2020). Theevolution of novel adsorbents with enhanced surface properties and adsorption capacities is crucial for improving the effectiveness of this technique. Currently, the substitution of artificial adsorbents with unconventional and economically viable materials has emerged as a focused area of study and development (Eletta *et al.* 2018). Consequently, many studies have been conducted on various methods to create inexpensive and promising adsorbents derived from biosorbents, natural resources, agricultural waste, and industrial residuals for the purpose of removing dyes from industrial effluent. These adsorbents have the potential to serve as a viable substitute for activated carbon (Demirbas, 2009; Yagub *et al.* 2014; Gimbert *et al.* 2008). The principal benefit of adsorption in the context of wastewater treatment is in its comparatively economical nature and robust efficacy in removing contaminants. Adsorbents effectively capture deleterious elements by means of intermolecular forces acting on the surface of the adsorbent material. Thus, additional treatment procedures are used to achieve thorough cleansing of water resources (Pan *et al.* 2020).

Nanocomposites, which integrate the distinctive characteristics of nanoparticles with traditional materials, are a highly promising category of adsorbents. The aforementioned materials frequently demonstrate augmented surface area, heightened porosity, and enhanced mechanical stability, rendering them very suitable for applications in environmental cleanup.In particular, the incorporation of metal oxides into clay matrices has shown significant potential for improving the adsorption of pollutants from water (Joshi *et al.* 2020). Stishovite, a high-pressure polymorph of silica with a tetragonal crystal structure, has been studied for its better thermal permanence, mechanical strength, and relatively high surface area, making it a potential substance for adsorption applications. Nevertheless, the adsorption capability of the material could be further improved by its combination with manganese dioxide (MnO_2), a metal oxide renowned for its exceptional adsorption and oxidative characteristics (Dong *et al.* 2013). The extensive application of MnO_2 in the elimination of organic pollutants andheavy metals can be attributed to its capacity to engage in redox reactions and establish robust surface complexes with contaminants (Anjum *et al.* 2023). This research presents the environmentally feasible production of a stishovite clay-MnO_2 nanocomposite specifically developed to function as anextremely efficient adsorbent for the elimination of dyes from industrial effluent. The synthesis approach prioritises environmental sustainability by eliminating the use of dangerous compounds and reducing energy consumption, in accordance with the concepts of green chemistry (Anastas and Warner, 1998; Tang *et al.* 2022). The research aims to contribute to the development of advanced materials for environmental remediation, specifically focusing on the elimination of hazardous dyes from wastewater. By leveraging the synergistic properties of stishovite clay and MnO_2 nanoparticles, this study seeks to offer a sustainable and efficient solution for dye pollution, thereby addressing a critical environmental challenge (Saleem and Zaidi, 2020).

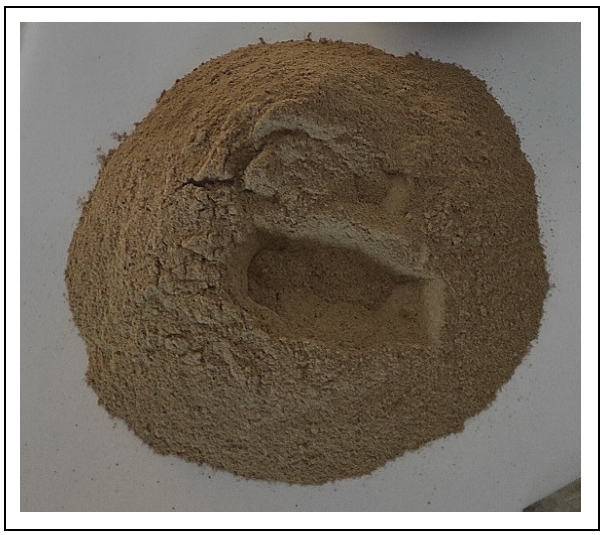

Fig. 1: Stishovite clay

2. MATERIALS

The materials utilized in this work were carefully chosen to validate the production of a high-quality, environmentally friendly nanocomposite with efficient dye elimination properties. Nanoparticles of Stishovite clay and manganese dioxide (MnO_2) are obtained from TEQTO Scientific Company in Coimbatore, India. Both materials function as the key constituents. The selection of Stishovite clay was based on its distinctive crystalline structure and exceptional surface area, which make it a very suitable foundation material for adsorption. The incorporation of MnO_2 nanoparticles was motivated by their intrinsic catalytic and adsorptive characteristics. To achieve the appropriate dispersion of the MnO_2 nanoparticles inside the clay matrix, ethanol was employed as a solvent during the synthesis procedure. Ethanol's low toxicity and facile elimination made it an appropriate option for this environmentally friendly synthesis technique. Purification and washing procedures were carried out using double-distilled water to guarantee the absence of impurities in all components and synthesised composites. Utilising double-distilled water ensured the

nanocomposite's highest level of purity, crucial for precise characterisation and dependable performance in following dye removal tests. Fig. 1 depicts the sample of Stishovite clay, shows its appearance and texture.

3. METHODS

3.1 Preparation of Stischovite Clay-Mno_2 Nanocomposite

The stischovite clay was rinsed with double distilled water to eradicatedirt and other impurities. Then, 15 g ofStishovite clay was dispersed in 75 ml of ethanol to for 3 hours at ambient temperature to get a homogeneous suspension. Then, 15 g of MnO_2 was mixed with 75 mL of ethanol. Following that, the diluted $MnO_2$was progressively disseminated into the clay suspension and agitated continuously for 7 hours at room temperature. Eventually, a 10mL volume of ethanol was combined with 1mL of distilled water and then gradually poured into the clay-MnO_2 matrix. Furthermore, the stirring process was carried out at ambient temperature for an additional period of six hours. Following centrifugation, the final suspension was repeatedly rinsed with double distilled water. Following a 24-hour drying period in a vacuum oven set at 90°C, the cleaned product was then cooled to room temperature. The desiccated composite was subsequently pulverized to a fine powder using a crusher or stone. The homogenous particle size was achieved by sieving the fine powder. The final product, which was designated as stischovite clay-MnO_2 nanocomposite, was stored in a sealed tight container for future use. While producing a high-quality, pure nanocomposite suitable for environmental remediation, this manufacturing process, which utilizes ethanol and double-distilled water, adheres to environmentally favourable standards by minimizing the use of harmful chemicals.

4. CHARACTERIZATION TECHNIQUES

The material characterization investigations were conducted at the STIC SAIF Analytical Division in Cochin, India.The structural, morphological, and chemical characteristics of the composite directly determine its efficacy as an adsorbent material for dye removal. The adsorptive behaviour and characteristics of Nano composites are determined through the application of numerous characterization techniques. Each analysis produces distinct findings, including determination of crystallinity, phase composition, surface morphology, and pore structure.

4.1 X-Ray Diffraction (XRD) Analysis

The crystallographic phase of stischovite clay and stischoviteclay-MnO_2 nanocomposites was identified using X-ray diffraction (XRD) analysis. The experimental protocol was carried out using a BRUKER AXS D8 ADVANCE X-ray diffractometer that was fitted with a copper anode and operated at a wavelength of 1.5406 Å. This instrument was capable of measuring the diffraction angle (2θ) within the range of 1° to 80º and was powered by a voltage of 40 kV and a current of 35 mA.

Fig. 2(a) and 2(b) show XRD examinations of Stishovite clay and Stishovite clay-MnO_2 nanocomposite, which demonstrate crystalline structures and variations in diffraction patterns after adding MnO_2.

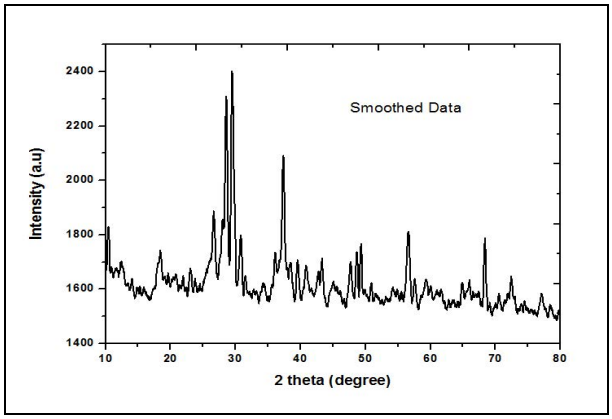

Fig. 2(a): XRD Analysis of stischovite clay

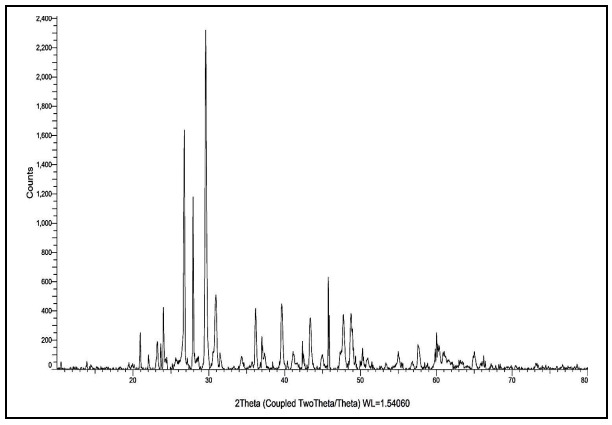

Fig. 2(b): XRD Analysis of stishovite clay - MnO_2 nanocomposite

The XRD configuration of the stishovite clay exhibits distinct peaks and indicates belonging to the tetragonal crystal structure. The existence of these distinct peaks verifies the integrity and crystalline structure of the stishovite clay, in the absence of any discernible contaminants or non-crystalline phases. Significant alterations were observed in the XRD pattern of the resulting nanocomposite after the integration of MnO_2 nanoparticles into the stishovite clay matrix. The nanocomposite exhibited the typical peaks of stishovite, but with diminished intensity and gradual broadening, suggesting a partial disturbance of the crystal lattice caused by the inclusion of MnO_2. Several new peaks associated with MnO_2 were detected in the XRD pattern,

providing confirmation of the effective amalgamation of MnO_2 into the clay matrix. The MnO_2-related peaks exhibited lower intensity in comparison to those of stishovite. This can be ascribed to the comparatively lower concentration of MnO_2 in the composite and its fine particle distribution within the clay matrix. The widening of these peaks indicates the presence of MnO_2 nanoparticles with fine crystallite dimensions, a characteristic feature of nanocomposites and beneficial for improving the adsorption surface area.

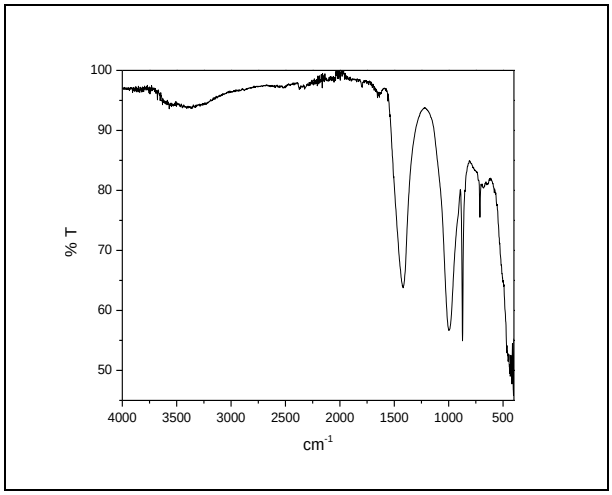

Fig. 3(a): FT-IR spectra for stischovite clay

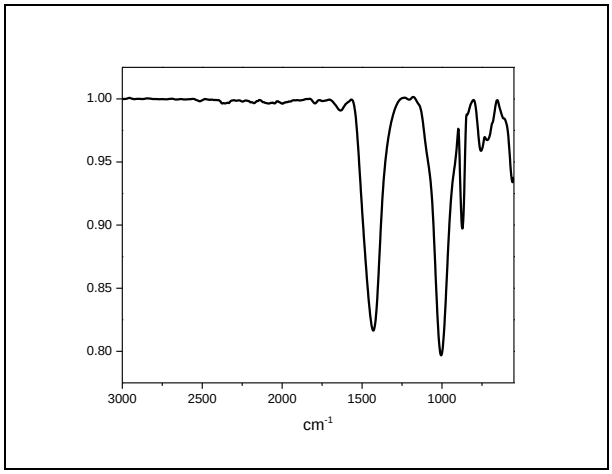

Fig. 3(b): FT-IR spectra for stishovite clay - MnO_2 nanocomposite

4.2 Fourier Transform Infrared (FT-IR) Analysis

The FT-IR spectra of stischovite clay and stischoviteclay-MnO_2 nanocomposites were examined to determine the existence of particular functional groups. The FT-IR spectrum observed ranged from 4000 - 400 cm-1. The AVATAR 370 spectrometer, which was manufactured by Thermo Nicolet, was employed to conduct the FT-IR analysis. This method entailed the exhaustive treatment of the powdered samples with solid KBr to produce thin pellets, which were subsequently employed for FT-IR examination. The FT-IR spectra of Stishovite clay and Stishovite-MnO_2 nanocomposite are shown in Figs. 3(a) and (b), which show the unique functional groups and changes in the chemical structure after MnO_2 is added.

The adsorption band in stischovite clay, which is situated between 3580-3690 cm^{-1}, is a result of the –OH stretching vibration of the water molecule (Cho *et al.* 2012). This band was relocated to 3710 cm-1 in the stischovite clay-MnO_2 nanocomposite. The twisting motion of the H-O-H group of water molecules adsorbed on the nanocomposite structure was found to be related with the band at 1665 cm^{-1} (Mariyam *et al.* 2021). Spectral peaks at 513.81 cm-1 are ascribed to the O-Mn-O and Mn-O vibrations (Mahmoud *et al.* 2022). The bending vibrations of the Si-O-AI and Si-O-Si clusters were detected at around 518.81 cm^{-1}. The Si-O-Si framework of the stishovite clay was preserved after the incorporation of MnO_2 nanoparticles, as evidenced by the FT-IR spectrum of the stishovite-MnO_2 nanocomposite, which exhibited analogous absorption bands. Nevertheless, the nanocomposite spectrum exhibited new absorption bands, particularly around 558.48 cm^{-1}, which are indicative of Mn-O vibrations, thereby confirming the presence of MnO_2 within the composite. The FT-IR analysis confirmed the presence of both stishovite clay and MnO_2 within the nanocomposite, with minimal degradation of the clay's structure and the successful integration of MnO_2.

4.3 Scanning Electron Microscope (SEM)

SEMillustrations of the samples using stischovite clay and The SEM images of Stishovite clay and Stishovite-MnO_2 nanocomposite are shown in Figs. 4(a) and 4(b), respectively, which illustrate the surface morphology and structural changes after MnO_2 incorporation.

The surface alterations observed in the stischovite clay-MnO_2 nanocomposite in comparison to stischovite clay.Stischovite clay was composed with a variation of irregular sizesand shapes of flakes, as well as damaged margins (Yadav *et al.* 2022). This clay has the ability to adhere to and stake on one another. This structure was compact and dense, suggesting a high level of crystallinity in the particles. This is a characteristic of natural clay materials, as the surface appeared to be flat with some minor porosity. Different non-clay variations can be found on the clay surface, indicated by the existence of certain white deposits in the mineral flakes. In the particle size (> 1 μm), the stischovite clay-MnO_2 nanocomposite exhibited a variety of shapes, including rough, bright, dispersed particles that were full of pore density, bends, flakes of varying sizes, and surface depression. In comparison to stischovite clay, this would suggest that the nanocomposite's surface area needs to be increased. The nanocomposite surface appeared to be

more porous and uncovered, which allowed for a greater degree of dye adsorption. The stishovite-MnO_2 nanocomposite exhibited substantial alterations in surface morphology when contrasted with the purified stishovite clay, as evidenced by the SEM images.

The surface was more heterogeneous and had a significant increase in surface roughness as a consequence of the incorporation of MnO_2 nanoparticles. Small, uniformly distributed concentrations of MnO_2 nanoparticles were observed on the surface of the stishovite clay particles. These nanoparticles contributed to a more porous and irregular surface, which is advantageous for improving the composite's adsorption capacity. An increase in surface area is indicated by the alteration in surface morphology, which is characterized by the formation of nanostructures. This increase is essential for the enhancement of the composite's adsorptive properties. The SEM analysis also verified the successful integration of MnO_2 into the stishovite clay matrix, as there were no visible indications of agglomeration, indicating that the nanoparticles were dispersed well.

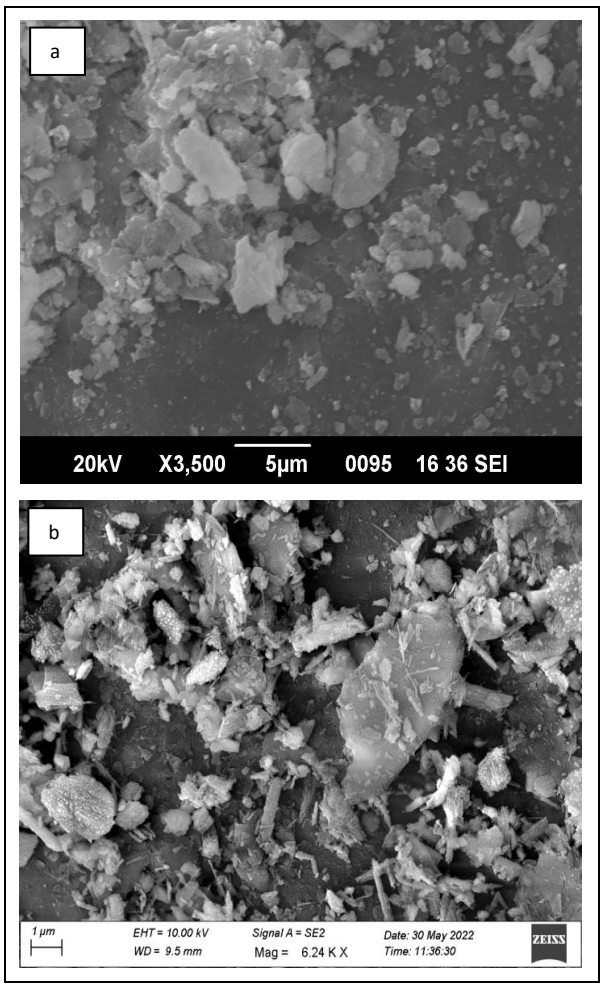

Fig. 4: (a) SEM Photograph for stischovite clay; (b) stishovite clay - MnO_2 nanocomposite

4.4 Energy Dispersive X-ray (EDX) Analysis

The elemental composition of the stishovite-MnO_2 nanocomposite was determined through the EDX analysis, which provided a comprehensive understanding of the material's elemental distribution. The nanocomposite's primary elements were Oxygen (23.3%), Manganese (21.2%), Silicon (10.1%), Aluminum (4.1%), Potassium (4.0%), and Magnesium (3.2%), as detected by the EDX spectrum. These results are in accordance with the composition anticipated from the synthesis process, which employed a 1:1 ratio of stishovite clay and MnO_2. Furthermore, the stishovite-MnO_2 nanocomposite's formation is further validated by the elemental ratios observed in the EDX analysis, which are reliable with the results of the XRD and FT-IR investigations. The uniform dispersion of MnO_2 within Stishovite clay is confirmed by the elemental distribution across the sample, as shown in Fig. 5. This uniformity is essential for the composite's efficacy as an adsorbent, as it guarantees that the active sites are uniformly distributed, thereby improving the material's overall performance in dye removal applications. The effective synthesis and characterization of the nanocomposite are strongly supported by the agreement between the EDX results and the XRD and FT-IR findings.

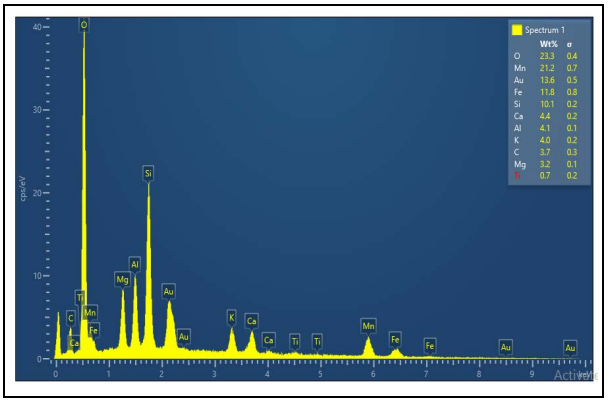

Fig. 5: EDX analysis stishovite clay -MnO_2 nanocomposite

4.5 Transmission Electron Microscopic Study (TEM)

The morphology of stischoite clay was determined through TEM analysis, which was subsequently modified with an equal proportion of MnO_2. The TEM images of Stishovite clay and Stishovite clay-MnO_2 nanocomposite are depicted in Figs. 6(a) and 6(b), respectively, which show the morphology and structural details of the samples.

The mesoporosity of stischovite clay was observed in Fig. 6(a) as a result of the formation of a clear density area within the stischovite clay crystallite following modification with an equal ratio of MnO_2. The 0.24nm lattice spacing ascribed to the plane was evidence

of the formation of MnO_2 particles on the surface of stischovite clay. The external surface of stichovite was the primary location of MnO_2 particles, as determined by TEM analysis.

Fig. 6(b) illustrates the SAED pattern observed on the stischovite clay-MnO_2 nanocomposite. The measured d-values are d1 = 8.24 1/nm and d2 = 14.05 1/nm. Undoubtedly, the consistent size of the pores was determined by the incorporation of the MnO_2 nanocomposite into the stischovite clay. Particle dimensions within the range of 19 to 54nm was established by determining the crystallite size using the XRD pattern. The stishovite-MnO_2 nanocomposite was characterised by TEM examination, revealing the presence of evenly distributed MnO_2 nanoparticles within the stishovite matrix. The uniform dispersion and nanoscale dimensions of the MnO_2 particles enhance the efficiency of the composite in dye removal applications by augmenting the surface area and producing a greater number of active sites for adsorption.

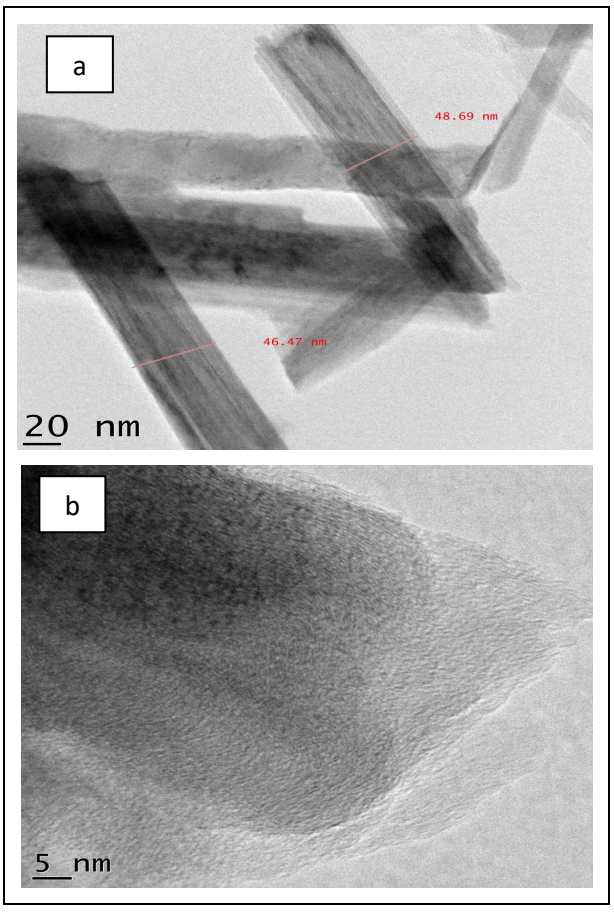

Fig. 6: (a) Tem analysis of stischovite clay; (b) Stishovite clay - MnO_2 nanocomposite

4.6Brunauer-Emmett-Teller (BET) Analysis

The specific surface area, pore diameter, and total volume of pores of the stishovite clay and the stishovite-MnO_2 nanocomposite have been assessed using a Brunauer-Emmett-Teller (BET) analysis.According to the IUPAC categorization system, the adsorbent displayed an isotherm of type IV and H3 hysteresis loop characteristics. Type H3 hyteresis loop is commonly observed in aggregates of plate-like particles that include slit-shaped holes. The first stage of the Type IV isotherm is linked to the single-layer-multilayer characteristics and describes the robust interactions between the adsorbate and the adsorbent surface. The isotherm arises from capillary condensation within mesopores.

Table 1. Pore and surface characteristics

Sample	Diameter of pore (nm)	Volume of pore (cm^3/g)	Surface area (m^2/g)
Stischovite clay	3.688	0.02	9.755
Stischovite clay-MnO_2 nanocomposites	3.646	0.046	18.583

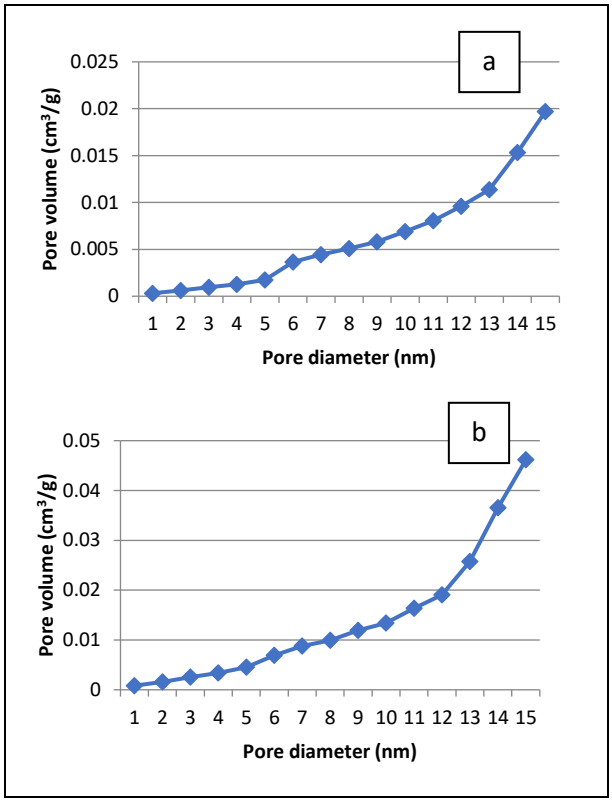

Fig. 7: (a) Pore volume distribution curves with pore diameter of the stichovite clay (b) Stischovite clay-MnO_2 nanocomposites

A hysteresis loop has been detected in the isotherm graph at high pressure, precisely when the ratio of P to Po is greater than 0.5. As the adsorption and desorption lines align in the low relative pressure range, it is possible that ink-bottle type holes are present. The

lesser quantities of N2 adsorbed at the low relative pressures provided evidence of the existence of dominating mesopores in the adsorbent topology. Furthermore, the presence of enhanced mesopores was indicated by the rise in adsorption inside the high relative pressure P/Po range, which is nearing 1.0.

Fig.7(a) depicts the pore diameters of Stishovite clay, while Fig.7(b) indicates that adding MnO_2 increases the pore volume, indicating that the material has more pores. This change indicates that adding MnO_2 enhances the porosity of the material. Table 1 compares the porosity and surface parameters of Stishovite clay and Stishovite clay-MnO_2 nanocomposites. The addition of MnO_2 results in a small structural variation, as the pore diameter reduces from 3.688 nm to 3.646 nm. The pore volume increases dramatically from 0.02 cm^3/g to 0.046 cm^3/g, whereas the surface area nearly doubles from 9.755 m^2/g to 18.583 m^2/g. Adding MnO_2 enhances the material's porosity and surface area; thus, it is ideal for applications like adsorption and catalysis that require high surface area and reactivity.

5. CONCLUSION

The subsequent inferences were arrived based on the experimental studies;

- In this investigation, a stishovite-MnO_2 nanocomposite was synthesized using environmentally friendly procedures and its properties were fully characterized.
- The crystalline nature of the stishovite clay and the incorporated MnO_2 nanoparticles was verified by the XRD analysis.
- The effective integration of MnO_2 into the stishovite matrix was confirmed by the FT-IR spectra.
- SEM and TEM images demonstrated a substantial alteration in surface morphology and the formation of nanoscale MnO_2 particles, which improved the composite's porosity and surface area.
- The BET analysis revealed a substantial increase in pore volume and surface area, which suggests that the adsorptive properties have been enhanced.
- The research findings revealed that the stishovite-MnO_2 nanocomposite has the potential to be an environmentally friendly and efficient material for environmental remediation. It exhibits improved properties that make it well-suited for applications such as dye removal.

FUNDING

This research received no specific grant from any funding agency in the public, commercial, or not-for-profit sectors.

CONFLICTS OF INTEREST

The authors declare that there is no conflict of interest.

COPYRIGHT

This article is an open-access article distributed under the terms and conditions of the Creative Commons Attribution (CC BY) license (http://creativecommons.org/licenses/by/4.0/).

REFERENCES

Adesanmi, B. M., Hung, Y. T., Paul, H. H. and Huhnke, C. R., Comparison of dye wastewater treatment methods: A review,*GSC Adv. Res. Rev.*, 10(2), 126–137 (2022). https://doi.org/10.30574/gscarr.2022.10.2.0054

Alahmadi, N., Recent progress in photocatalytic removal of environmental pollution hazards in water using nanostructured materials, *Sep.*, 9(10), 264 (2022). https://doi.org/10.3390/separations9100264

Al-Tohamy, R., Ali, S. S., Li, F., Okasha, K. M., Mahmoud, Y. A. G., Elsamahy, T., Jiao, H., Fu, Y. and Sun, J., A critical review on the treatment of dye-containing wastewater: Ecotoxicological and health concerns of textile dyes and possible remediation approaches for environmental safety,*Ecotoxicol. Environ. Saf.*, 231, 113160 (2022). https://doi.org/10.1016/j.ecoenv.2022.113160

Anastas, P. T. and Warner, J. C., *Green Chemistry: Theory and Practice*, Oxford University Press (1998).

Anjum, M., Liu, W., Qadeer, S. and Khalid, A., Photocatalytic treatment of wastewater using nanoporous aerogels: Opportunities and challenges, *Emerg. Technol. Treat. Toxic Metals Wastewater*, 495–523. Elsevier (2023). https://doi.org/10.1016/B978-0-12-822086-7.00024-2

Arunvivek, G. K., Preetha, A., Bragadeeswaran, T. and Mahendran, D., Study on Behavior of Paper Industry Treated Effluent as Mixing Water in Concrete for Pollution Control and Sustainable Development. *Int. J. Eng. Res. Technol.*, 3(8), 1049–1051 (2014).

Benkhaya, S., M'rabet, S., Hsissou, R. and El Harfi, A., Synthesis of new low-cost organic ultrafiltration membrane made from Polysulfone/Polyetherimide blends and its application for soluble azoic dyes removal,*J. Mater. Res. Technol.*, 9(3), 4763–4772 (2020). https://doi.org/10.1016/j.jmrt.2020.02.102

Cardona, Y., Węgrzyn, A., Miśkowiec, P., Korili, S. A. and Gil, A., Catalytic photodegradation of organic compounds using TiO2/pillared clays synthesized using a nonconventional aluminum source, *Chem. Eng. J.*, 446, 136908 (2022). https://doi.org/10.1016/j.cej.2022.136908

Chitradevi, R., Jeyaraj, M., Ghadamode, V. D., Poonkodi, K., Venkadasamy, R. andMagudeswaran, P. N., Assessment of water quality using modified water quality index and geographical information system in Madathukulam Taluk, Tiruppur District, Tamil Nadu, India, *Orient. J. Chem.*, 37(5), 1210–1220 (2021). https://doi.org/10.13005/ojc/370528

Cho, D. W., Jeon, B. H., Chon, C. M., Kim, Y., Schwartz, F. W., Lee, E. S. and Song, H., A novel chitosan/clay/magnetite composite for adsorption of Cu (II) and As (V), *Chem. Eng. J.*, 200, 654–662 (2012). https://doi.org/10.1016/j.cej.2012.06.126

Demirbas, A., Agricultural based activated carbons for the removal of dyes from aqueous solutions: A review, *J. Hazard. Mater.*, 167(1–3), 1–9 (2009). https://doi.org/10.1016/j.jhazmat.2008.12.114

Dong, W., Zang, L. and Li, H., Application of MnO2 materials to dye removal from aqueous solution by adsorption, *Appl. Mech. Mater.*, 361-363, 760–763 (2013). https://doi.org/10.4028/www.scientific.net/AMM.361-363.760

Ebrahimi, F., Nabavi, S. R. and Omrani, A., Fabrication of hydrophilic hierarchical PAN/SiO2 nanofibers by electrospray assisted electrospinning for efficient removal of cationic dyes, *Environ. Technol. Innov.*, 25, 102258 (2022). https://doi.org/10.1016/j.eti.2021.102258

El-Kassimi, A., Achour, Y., El Himri, M., Laamari, M. R. and El Haddad, M., High efficiency of natural Safiot clay to remove industrial dyes from aqueous media: Kinetic, isotherm adsorption and thermodynamic studies,*Biointerface Res. Appl. Chem.*, 11(5), 12717–12731 (2021). https://doi.org/10.33263/BRIAC115.1271712731

Eletta, O. A. A., Mustapha, S. I., Ajayi, O. A. and Ahmed, A. T., Optimization of dye removal from textile wastewater using activated carbon from sawdust, *Niger. J. Technol. Dev.*, 15(1), 26 (2018). https://doi.org/10.4314/njtd.v15i1.5

Garg, S. K. and Tripathi, M., Microbial strategies for discoloration and detoxification of azo dyes from textile effluents. *Res. J. Microbiol.*, 12, 1–19 (2017). https://doi.org/10.3923/jm.2017.1.19

Gimbert, F., Morin-Crini, N., Renault, F., Badot, P. M. and Crini, G., Adsorption isotherm models for dye removal by cationized starch-based material in a single component system: Error analysis, *J. Hazard. Mater.*, 157(1), 34–46 (2008). https://doi.org/10.1016/j.jhazmat.2007.12.072

Gupta, V. K. and Suhas., Application of low-cost adsorbents for dye removal – A review, *J. Environ. Manage.*, 90(8), 2313–2342 (2009). https://doi.org/10.1016/j.jenvman.2008.11.017

Ismadji, S., Shen, D., Edi, F., Ayucitra, A., Hua, W. and Hui, C., Bentonite hydrochar composite for removal of ammonium from Koi fish tank, *Appl. Clay Sci.*, 119(1), 146-154 (2016). https://doi.org/10.1016/j.clay.2015.08.022

Jana, S., Ray, J., Mondal, B. and Tripathy, T., Efficient and selective removal of cationic organic dyes from their aqueous solutions by a nanocomposite hydrogel, katira gum-cl-poly (acrylic acid-co-N, N-dimethylacrylamide)@bentonite, *Appl. Clay Sci.*, 173, 46–64 (2019). https://doi.org/10.1016/j.clay.2019.03.009

Januário, E. F. D., Vidovix, T. B., Bergamasco, R. and Vieira, A. M. S., Performance of a hybrid coagulation/flocculation process followed by modified microfiltration membranes for the removal of Solophenyl Blue dye,*Chem. Eng. Process. Process Intensif.*, 168, 108577 (2021). https://doi.org/10.1016/j.cep.2021.108577

Joshi, P., Gupta, K., Gusain, R. and Khatri, O., Metal oxide nanocomposites for wastewater treatment, *Adv. Water Treat. Environ. Manage.*, 283–314. Wiley (2020). https://doi.org/10.1002/9781119364726.ch11

Khan, S. H. and Pathak, B., Zinc oxide-based photocatalytic degradation of persistent pesticides: A comprehensive review, *Environ. Nanotechnol. Monit. Manag*, 13, 100290 (2020). https://doi.org/10.1016/j.enmm.2020.100290

Kishor, R., Purchase, D., Saratale, G. D., Saratale, R. G., Ferreira, L. F. R., Bilal, M., Chandra, R. andBharagava, R. N., Ecotoxicological and health concerns of persistent coloring pollutants of textile industry wastewater and treatment approaches for environmental safety, *Environ. Chem. Eng.*, 9, 105012 (2021). https://doi.org/10.1016/j.jece.2020.105012

Lou, Z., Li, R., Liu, J., Wang, Q., Zhang, Y. and Li, Y., Used dye adsorbent derived N-doped magnetic carbon foam with enhanced electromagnetic wave absorption performance, *J. Alloys Compd.*, 854, 157286 (2021). https://doi.org/10.1016/j.jallcom.2020.157286

Mahmoud, M. E., Amira, M. F., Azab, M. M. H. M. and Abdelfattah, A. M., An innovative aminomagnetite@grapheneoxide@amino-manganese dioxide as a nitrogen-rich nanocomposite for removal of Congo red dye, *Diam. Relat. Mater.*, 121, 108744 (2022). https://doi.org/10.1016/j.diamond.2021.108744

Mariyam, A., Mittal, J., Sakina, F., Baker, R. T., Sharma, A. K. and Mittal, A., Efficient batch and fixed-bed sequestration of a basic dye using a novel variant of ordered mesoporous carbon as adsorbent, *Arab. J. Chem.*, 14(6), 103186 (2021). https://doi.org/10.1016/j.arabjc.2021.103186

Moneer, A. A., El-Mallah, N. M., Ramadan, M. S. and Shaker, A. M., Removal of Acid Green 20 and Reactive Yellow 17 dyes by aluminum electrocoagulation technique in a single and a binary dye system, *Egypt. J. Aquat. Res.*, 47(2), 223–230 (2021). https://doi.org/10.1016/j.ejar.2021.04.004

Mudhoo, A., Ramasamy, D. L., Bhatnagar, A. A., Usman, M. and Sillanpaa, M., An analysis of the versatility and effectiveness of composts for sequestering heavy metal ions, dyes, and xenobiotics from soils and aqueous milieus, *Ecotoxicol. Environ. Saf.*, 197, 110587 (2020). https://doi.org/10.1016/j.ecoenv.2020.110587

Pan, D., Ge, S., Tian, J., Shao, Q., Guo, L., Liu, H., Wu, S., Ding, T. and Guo, Z., Research progress in the field of adsorption and catalytic degradation of sewage by hydrotalcite-derived materials, *Chem. Rec.*, 20(4), 355–369 (2020). https://doi.org/10.1002/tcr.201900071

Parmar, S., Daki, S., Bhattacharya, S. and Shrivastav, A., Microorganism: An eco-friendly tool for waste management and environmental safety, *Dev. Wastewater Treat. Res. Process.*, 175–193. Elsevier (2022). https://doi.org/10.1016/B978-0-323-85657-7.00001-8

Raval, R., Kohli, H. P. and Mahadwad, O. K., Application of emulsion liquid membrane for removal of malachite green dye from aqueous solution: Extraction and stability studies, *Chem. Eng. J. Adv.*, 12, 100398 (2022). https://doi.org/10.1016/j.ceja.2022.100398

Roa, K., Oyarce, E., Boulett, A., ALSamman, M., Oyarzún, D., Pizarro, G. D. C. and Sánchez, J. Lignocellulose-based materials and their application in the removal of dyes from water: A review. *Sustain. Mater. Technol.*, 29, e00320 (2021). https://doi.org/10.1016/j.susmat.2021.e00320

Saad, A. and Atia, A., Review on freshwater blue-green algae (cyanobacteria): occurrence, classification and toxicology,*Biosci. Biotechnol. Res. Asia*, 11, 1319–1325 (2014). https://doi.org/10.13005/bbra/1522

Saleem, H. and Zaidi, S. J., Developments in the application of nanomaterials for water treatment and their impact on the environment, *Nanomater.*, 10(9), 1764 (2020). https://doi.org/10.3390/nano10091764

Shajeelammal, J., Mohammed, S., Prathish, K. P., Jeeva, A., Asok, A. and Shukla, S., Advances in treatment of real-time textile effluent containing azo reactive dyes via ozonation, modified pulsed low frequency ultrasound cavitation, and integrated reactor, *J. Hazard. Mater. Adv.*, 7, 100098 (2022). https://doi.org/10.1016/j.hazadv.2022.100098

Talaiekhozani, A., Mosayebi, M. R., Fulazzaky, M. A., Eskandari, Z. and Sanayee, R., Combination of TiO2 microreactor and electroflotation for organic pollutant removal from textile dyeing industry wastewater, *Alex. Eng. J.*, 59(2), 549–563 (2020). https://doi.org/10.1016/j.aej.2020.01.052

Tang, Z., Ma, D., Chen, Q., Wang, Y., Sun, M., Lian, Q., Shang, J., Wong, P. K., He, C. and Xia, D., Nanomaterial-enabled photothermal-based solar water disinfection processes: Fundamentals, recent advances, and mechanisms, *J. Hazard. Mater.*, 437, 129373 (2022). https://doi.org/10.1016/j.jhazmat.2022.129373

Xiang, J., Wang, X., Ding, M., Tang, X., Zhang, S., Zhang, X. and Xie, Z., The role of lateral size of MXene nanosheets in membrane filtration of dyeing wastewater: Membrane characteristic and performance, *Chemosphere*, 294, 133728 (2022). https://doi.org/10.1016/j.chemosphere.2022.133728

Yadav, A., Bagotia, N., Yadav, S., Sharma, A. K. and Kumar, S., Adsorptive studies on the removal of dyes from single and binary systems using Saccharummunja plant-based novel functionalized CNT composites, *Environ. Technol. Innov.*, 24, 102015 (2021). https://doi.org/10.1016/j.eti.2021.102015

Yadav, M., Thakore, S. and Jadeja, R., Removal of organic dyes using Fucus vesiculosus seaweed bioadsorbent: An ecofriendly approach, *Environ. Chem. Ecotoxicol.*, 4, 67–77 (2022). https://doi.org/10.1016/j.enceco.2021.12.003

Yagub, M. T., Sen, T. K., Afroze, S. and Ang, H. M., Dye and its removal from aqueous solution by adsorption: A review, *Adv. Coll. Int. Sci.*, 209, 172–184 (2014). https://doi.org/10.1016/j.cis.2014.04.002

Younis, S. A., Serp, P. S. and Nassar, H. N., Photocatalytic and biocidal activities of ZnTiO2 oxynitrite heterojunction with MOF-5 and G-C3N4: A case study for textile wastewater treatment under direct sunlight, *J. Hazard. Mater.*, 410, 124562 (2021). https://doi.org/10.1016/j.jhazmat.2021.124562

Zhao, B., Zhao, Y., Liu, P., Men, Y. L. and Pan, Y. X., Degradation of organic dyes by hierarchical porous carbon derived from iron-containing biomass, *Chem. Eng. J.*, 443, 136290 (2022). https://doi.org/10.1016/j.cej.2022.136290

Zupko, R., Kamath, D., Coscarelli, E., Rouleau, M. and Minakata, D., Agent-based model to predict the fate of the degradation of organic compounds in the aqueous-phase UV/H2O2 advanced oxidation process, *Process Saf. Environ. Prot.*, 136, 49–55 (2020). https://doi.org/10.1016/j.psep.2020.01.023